

DCS F-100D Super Sabre: Flight Model and Methodology 2

Abstract—This report presents a comprehensive flight model simulation methodology incorporating large-scale wind tunnel testing and real-world aerodynamic coefficient data to achieve high-fidelity simulation. The simulation utilizes experimentally derived coefficients of lift, drag, and moment, ensuring accuracy through comparison with flight performance charts and dynamic response data. Key deliverables included are coefficient of lift plots, flight envelopes, stall speed determinations, glide performance charts, fuel consumption analysis, excess power assessments, turn rate evaluations, and comprehensive performance charts. These outputs provide a detailed understanding of the module's accuracy.

1. Concept Development

The F-100D Super Sabre initially did not appear to have much raw coefficient data. After further review, the aircraft was mentioned as a *45 degree swept-wing fighter type design* in historical reports. Figure 1 shows what resembles an F-100 series aircraft with different tail sizing. NACA RM L55F21 [10] is the result of testing larger tail designs, similar to the F-100D. Thus, our flight model base is built upon this collection of NACA research documents. Namely, NASA MEMO 10-1-58H [1], NACA RM H55A13 [7], NACA RM H56C20 [8], and NACA RMH 56H03 [9].

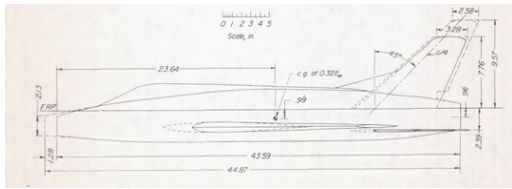


Figure 1. Example of 0.0825 scale wind tunnel model from NACA RM L55F21 [10].

Later, this base was tested with real world F-100D specific dynamic response and performance data.

2. Non-Linear Simulation Tool Overview

Results were produced using an in-house nonlinear simulation tool. Our tool uses open source physics libraries and flight model data to produce forces and moments for each simulation frame faster than real time simulation. We have compared our results to DCS results in order to validate the simulation tool output. The tool is commanded by scripted test cases that can produce outputs for any test needed in seconds. Batch testing is also possible in order to produce a set of tests together. Thus, each test is perfectly repeatable as to track changes after data updates easily holistically throughout the flight model.

3. Aerodynamics

3.1. Lift Curve

The lift curve was first generated from computational methods and then cross referenced with our references. The TAC ATTACK Publication [5] details in depth handling qualities with angle of attack (AOA), specifically AOA for minimum control and stall. With the F-100D-1 [4] stall speed table we were satisfied with our lift curve $C_{L,MAX}$ and $C_{L,MINCONTROL}$. The rest of the lift curve was built out using first principles aerodynamics, our two known points, and computational methods.

Figure 2 shows $C_{L,MAX}$ as compared to Mach.

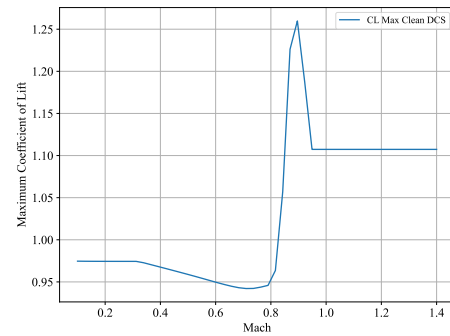


Figure 2. $C_{L,MAX}$ vs Mach.

Subsonic stall speeds match closely with real data. Transonic $C_{L,MAX}$ of roughly 1.269 was calculated from stall AoA and $C_{L,a}$ at mach 0.9 and 1.12 and mach 1.15.

Figure 3 shows C_L as compared to AOA for both the clean and dirty configuration at different mach numbers.

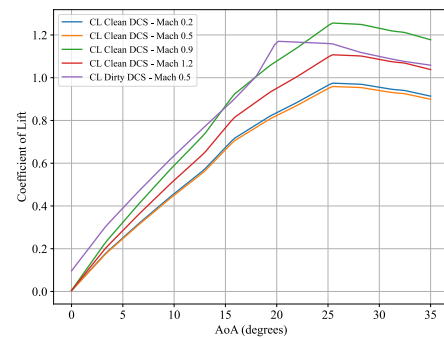


Figure 3. C_L vs AOA.

4. Static Stability Analysis

4.1. Loading

Although the only relevant factor for the flight model is the location of the forces compared to the center of gravity (CG), we wanted to guarantee that the loading scheme of the aircraft was close to the real world counterpart. This would ensure that our fuel tanks filled accurately and thus we could use the CG location for development of stability with different loading, using the CG as the index.

With medium confidence, we were able to take CG values with aircraft weight for known clean configurations and loaded configurations. This is medium confidence because it is unknown what other factors contributed to the loading other than the load out. Figure 4 shows that the trend of loading is correct and within an acceptable error margin. Thus, we were satisfied with the results.

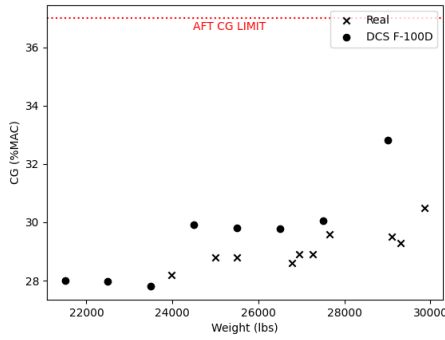


Figure 4. Real loading scheme vs DCS F-100D.

Furthermore, we produced numbers for Static Margin (SM) and the Neutral Point (NP). Neutral Point and Center of Gravity were verified with NACA RMH 56H03 [9] using flight derived data for $C_{L,\alpha}$ and $C_{m,\alpha}$. These parameters are purely for tracking and validation purposes (as forces are centered and moments are added separately). Figure 5 shows the trend of SM and CG with both fuel load and aircraft weight.

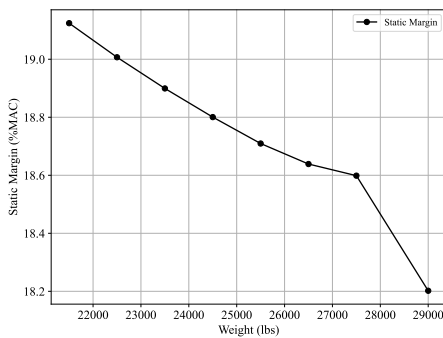


Figure 5. Static Margin.

Table 1 shows an example calculation of the aircraft stability parameters at 29,000 lbs. Note: NP is the aerodynamic center and does not change with weight.

Table 1. Stability parameters at 29,000 lbs

Parameter	%MAC	Feet Aft of Datum
Center of Gravity	29.5	22.6
Neutral Point	41.0	23.8
Static Margin	11.5	1.28 length

Note: CG and SM change with weight. $SM = NP - CG$

The above values are only used as references and arguments to select or blend coefficients to adjust for handling qualities based on loading. Validation of these handling qualities are based on weight; thus, the accuracy of the loading scheme serves no real importance of flight model accuracy and is merely for use as described.

4.2. Longitudinal Stability

Figure 6 shows the aircraft's clean neutral trim point as a function of Mach and elevator, δ_e . Lines are shown for both the forward and after CG limits.

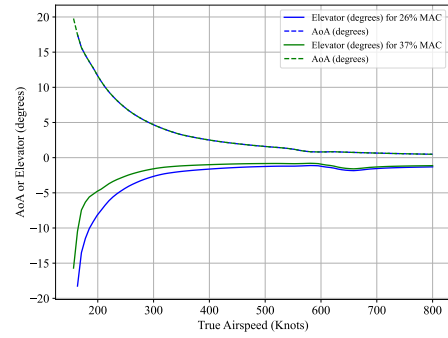


Figure 6. Trim plot for clean and dirty configurations.

4.3. Lateral Directional Stability

The roll rate of the aircraft is the neutral rolling moment condition. We have replicated the test from AD No. 152258 [2] Figure 126, 128, and 129.

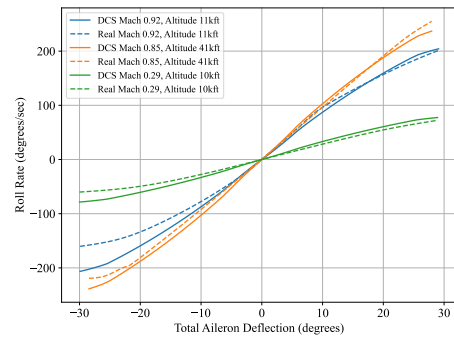


Figure 7. Roll rate for clean and dirty configurations.

5. Dynamic Stability Analysis

5.1. Longitudinal Stability

Longitudinal response tests were replicated from AD No. 152258 [2] Figure 78.

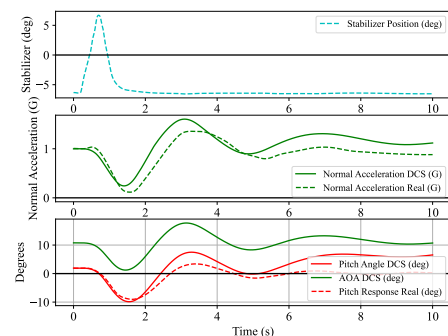


Figure 8. Response to nose down stick wrap, dirty M=0.326.

More dynamics response tests are listed in appendix A.

5.2. Lateral Directional

Lateral directional response tests were replicated from AD No. 152258 [2] Figure 116.

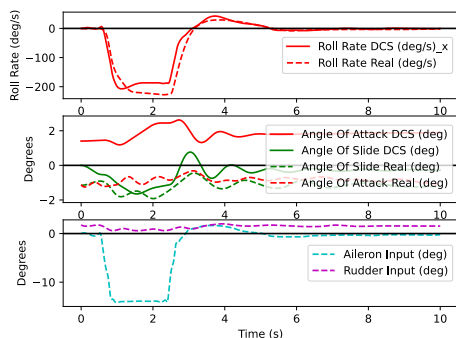


Figure 9. Response to step aileron input.

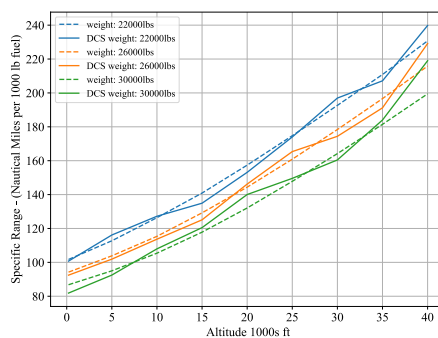


Figure 10. Specific Range.

6. Performance

The F-100D performance supplement [3] was used to validate the flight model’s in-game fidelity. These tests included the nonlinear simulation tool and in game test flights for takeoff and landing distances, fuel (endurance and range), stall speeds, excess specific power, and Turn Rate.

6.1. Takeoff and Landing Distance

Takeoff and landing distances were mostly derived from in-game flight tests to capture the full effects of the Eagle Dynamics suspension and friction model. Below are tables that show the DCS F-100D takeoff and landing distances as compared to the real aircraft for varying weights.

Table 2. Takeoff distance

Weight(lbs)	DCS(ft)	Real(ft)/Speed(KIAS)
24,000	1,956	2,000/153
26,000	2,246	2,225/156
28,000	2,511	2,510/158
34,000	3,553	3,590/167

Table 3. Landing distance

Weight(lbs)	DCS(ft)	Real(ft)
24,000	5,003	4,400
26,000	5,216	4,750
28,000	5580	5230
34,000	6300	6050

6.2. Fuel Performance

Figure 10 shows the specific range in relation to altitude at different weights. The data were compared to the real aircraft from the F-100D Performance Supplement [3].

6.3. Stall Speed

Stall speeds are defined as 20 degrees AOA while minimum controllable airspeed is defined as 18 degrees by the TAC ATTACK [5] publication in the dirty configuration. Using these data points combined with the stall speed table in the F-100D-1 [4] we confidently reproduced an accurate lift curve slope for the dirty configuration that satisfied all stall speeds at a high degree of accuracy, as shown in Figure 11.

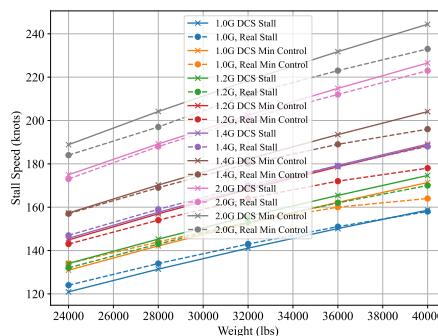


Figure 11. Dirty stall speeds.

With computational modeling we were able to back calculate the clean configuration lift curve slope and approximate stall angle that satisfied our references, which are shown in Figure 12.

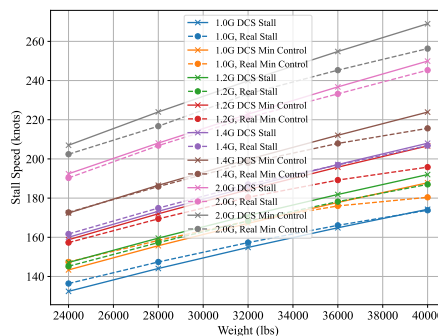


Figure 12. Clean stall speeds.

6.4. Excess Specific Power

Excess power tests from AD0372500 [6] figure were replicated for multiple altitudes. Figure 13 shows a sample of the comparison between DCS and the real data for sea level.

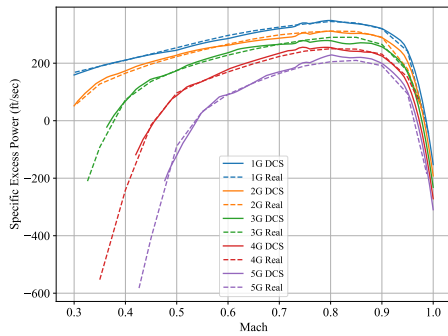


Figure 13. Seal level excess power max thrust.

More tests at different power settings and pressure altitudes can be found in appendix B.

6.5. Performance Envelope

The F-100D Performance Envelope as a result from DCS is shown below. This shows the max speed and stall speed as a function of Mach. Note that it is unclear what is defined as the accelerated stall line given that this is a swept wing airplane with no defined stall. We referenced the previous TAC Attack [5] AOA numbers discussed, but this necessarily does not coincide with the same parameters used to generate the diagram.

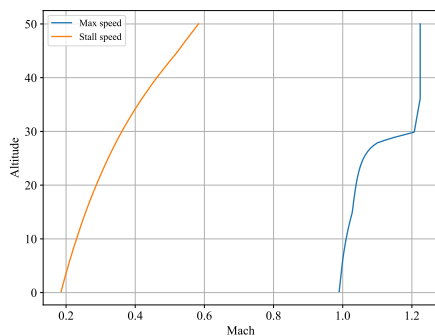


Figure 14. Performance envelope.

6.6. Glide

None of the data sources provide data for the F-100D gliding performance with a windmilling engine. Given that our other performance data matches closely we can confidently conclude our glide performance is at a high degree of confidence shown below in Figure 15.

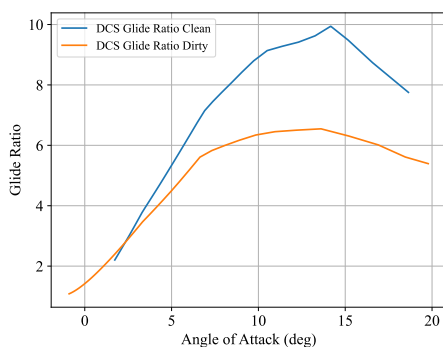


Figure 15. Glide ratio as a function of AOA under windmilling condition.

Figure 16 shows the gliding vertical velocity as a function of true airspeed under a windmilling condition.

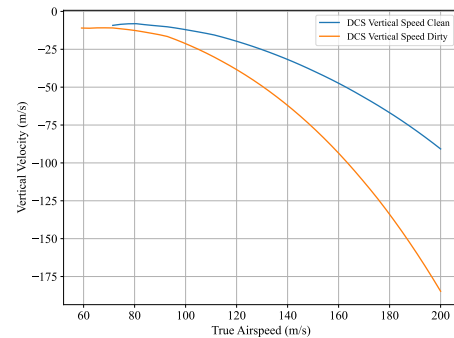


Figure 16. Gliding vertical velocity as a function of true airspeed.

7. Results and Future Improvements

We are pleased with the current accuracy of the DCS F-100D flight model as it currently stands. In aerodynamics, stability and control, dynamics, and performance, our flight model has achieved a high degree of accuracy as compared to real-world data that we have obtained. However, we have identified a few key areas for improving the flight model in future releases. As a note, it is important to remember that we have little reference to the methodology of our data. As our data are a collection of many different reports, the methodology is not consistent and we expect to see further mismatches in our data as compared to real world data. Thus, it is impossible to match every data chart exactly as tuning of one test point may influence the results of another. However, we aim to achieve a high degree of accuracy in our test replications that match every test point as closely as possible overall.

In terms of static and dynamic stability, we will continue to monitor accuracy with our limited charts for different loading scenarios. Further improvements can be made to match static stability charts in both longitudinal and lateral directional. Specifically, for dynamic stability we can further match frequency, period, and natural frequency of the response modes.

Performance wise, we aim to greatly improve our flight envelope to further match the results from the changes in altitudes. Moreover, our excess power is generally accurate, but we will greatly be improving the lower end and farther end of the load factor excess power lines as our middle range load factors are accurate.

It is important to note that many of the above tests cannot be used to conclude inaccuracies. We do not have full details and assumptions for the real-world tests. Moreover; our assumptions for static and dynamic stability tests were a 1G straight and level unaccelerated flight condition at zero vertical airspeed. Our tests then placed the aircraft at an equivalent nose attitude to the real world counterpart's initial conditions. As these were our assumptions, lack of the aircraft's nose tracking with real-world tests is inconsequential conclusions to the level of accuracy. Measurements with a potential for accumulated error should only be noted for trend, phase, and amplitude accuracy while instantaneous measurements are of higher importance.

References

- [1] N. M. 10-1-58H, *Lift and drag of a swept-wing fighter airplane at transonic and supersonic speeds.*
- [2] A. N. 152258, *Arc f-100d category ii performance stability and control tests.*
- [3] T. 1F-100A-1-1, *Performance data usaf series f100 acdf aircraft.*
- [4] T. 1F-100A(1)-1, *Flight manual usaf series f-100d.*

- [5] T. 69-07, Tac attack sabre and angles.
- [6] DTIC, Ad0372500 air combat tactics evaluation f-100, f-104, f-105, f-4c vs mig-15/17 type a/c(f-86h).
- [7] N. R. H55A13, Flight experience with two high-speed airplanes having violent lateral-longitudinal coupling in aileron rolls.
- [8] N. R. H56C20, Time-vector determined lateral derivatives of a swept-wing fighter-type airplane with three different vertical tails at mach numbers between 0.70 and 1.48.
- [9] N. R. H56H03, Dynamic longitudinal stability characteristics of a swept-wing fighter-type airplane at mach numbers between 0.36 and 1.45 .
- [10] N. R. L55F21, Wind-tunnel investigation at low speed of sideslipping, rolling, yawing, and pitching characteristics for a model of a 450 swept-wing fighter-type airplane.

A. Dynamic Response Appendix

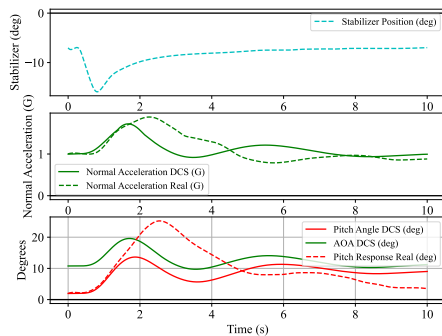


Figure 17. Response to nose up stick wrap, dirty M=0.326.

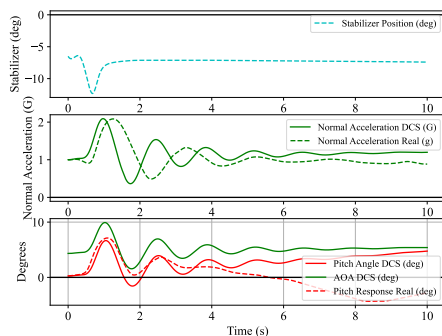


Figure 18. Response to up down stick wrap, M=0.9.

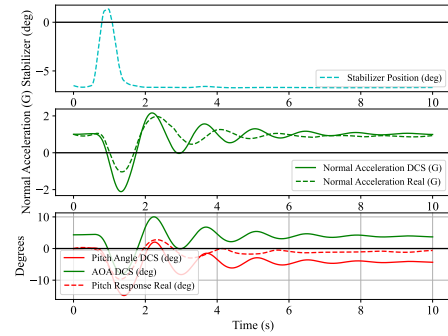


Figure 19. Response to nose down stick wrap, M=0.9.

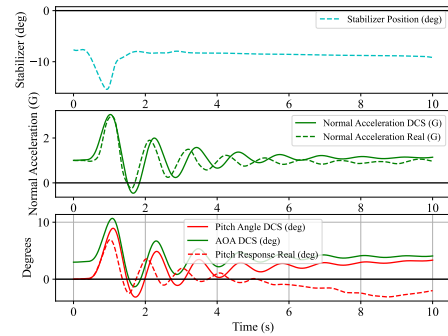


Figure 20. Response to nose down stick wrap, M=1.105.

B. Excess Power Appendix

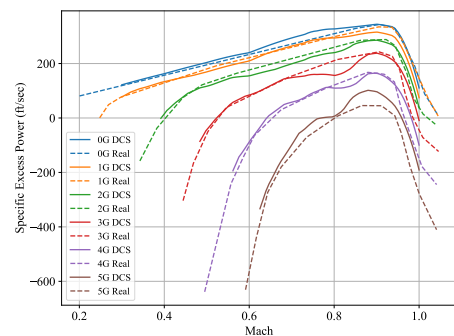


Figure 21. 15,000 ft excess power max thrust.

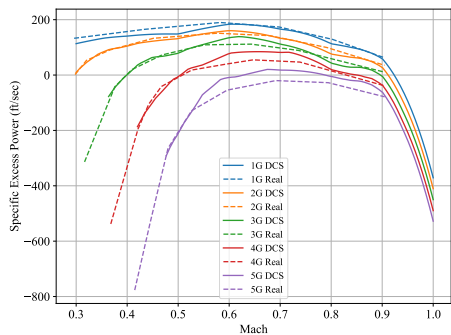


Figure 22. Seal level excess power military thrust.

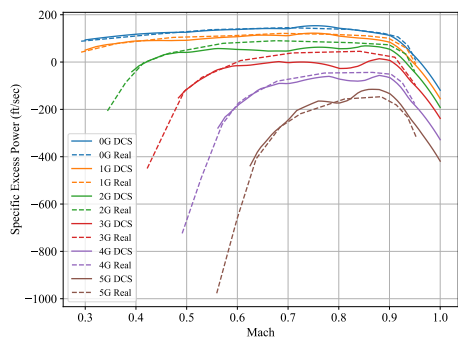


Figure 23. 15,000 ft excess power military thrust.